

Nonlinear Mathematical Simulation and Analysis of *Dha* Regulon for Glycerol Metabolism in *Klebsiella pneumoniae**

SUN Yaqin (孙亚琴)¹, YE Jianxiong (叶剑雄)², MU Xiaojia (牟晓佳)¹, TENG Hu (滕虎)¹, FENG Enmin (冯恩民)², ZENG Anping (曾安平)³ and XIU Zhilong (修志龙)^{1,**}

¹ Department of Bioscience & Biotechnology, Dalian University of Technology, Dalian 116024, China

² Department of Applied Mathematics, Dalian University of Technology, Dalian 116024, China

³ Institute of Bioprocess and Biochemical Engineering, Technical University of Hamburg-Harburg, D-21073 Hamburg, Germany

Abstract Glycerol may be converted to 1,3-propanediol (1,3-PD) by *Klebsiella pneumoniae* under anaerobic conditions and glycerol dismutation involves two parallel pathways controlled by the *dha* regulon. In this study, a fourteen-dimensional nonlinear dynamic system is presented to describe the continuous culture and multiplicity analysis, in which two regulated negative-feedback mechanisms of repression and enzyme inhibition are investigated. The model describing the expression of gene-mRNA-enzyme-product was established according to the repression of the *dha* regulon by 3-hydroxypropionaldehyde (3-HPA). Comparisons between simulated and experimental results indicate that the model can be used to describe the production of 1,3-PD under continuous fermentation. The new model is translated into the corresponding S-system version. The robustness of this model is discussed by using the S-system model and the sensitivity analysis shows that the model is sufficiently robust. The influences of initial glycerol concentration and dilution rate on the biosynthesis of 1,3-PD and the stability of the *dha* regulon model are investigated. The intracellular concentrations of glycerol, 1,3-PD, 3-HPA, repressor mRNA, repressor, mRNA and protein levels of glycerol dehydratase (GDHt) and 1,3-PD oxydoreductase (PDOR) can be predicted for continuous cultivation. The results of simulation and analysis indicate that 3-HPA accumulation will repress the expression of the *dha* regulon at the transcriptional level. This model gives new insights into the regulation of glycerol metabolism in *K. pneumoniae* and explain some of the experimental observations.

Keywords *dha* regulon, robustness, nonlinear dynamics, genetic regulation, 3-hydroxypropionaldehy

1 INTRODUCTION

The purpose of systems biology is not to build the system from its molecular components, but to build subsystems from molecules and the system from these subsystems [1]. The current rapid development of genomic data has attracted much more attention to the regulation of gene expression and its products, mRNAs and proteins under biological system [2]. The complex mechanisms of genes regulation might lead to biodiversity and nonlinear phenomena.

The bioconversion of glycerol to 1,3-propanediol (1,3-PD) has recently received more interest because of the industrial utilization of 1,3-PD especially as a monomer of polyesters, and polyurethanes [3]. Glycerol is a low-cost renewable resource appearing in increasing quantities as the principal by-product from fat saponification, alcoholic beverage and bio-diesel production facilities [4, 5]. Biodiesel is produced by the transesterification of plant seed oils, which yields glycerol as the main by-product (about 10% by mass). About 50% of the entire cost of the microbial production of 1,3-propanediol is due to the price of raw materials [6]. The economical viability of this process is dependent on the price and availability of glycerol. As a carbon feedstock for fermentations, glycerol could be competitive if its price is not more than US\$ 0.3

per kg [7]. Glycerol utilization for cell growth operates through two systems in *Klebsiella pneumoniae*. In the presence of exogenous electron acceptors the dissimilation is governed by the *glp* regulon. However, under anaerobic conditions glycerol dismutation involves two parallel pathways regulated by the *dha* regulon where oxidative and reductive pathways are coupled. In the oxidative pathway glycerol is oxidized to dihydroxyacetone (DHA) by the enzyme glycerol dehydrogenase (GDH) and this step is coupled to the reducing equivalent formation for the reductive pathway. DHA is further phosphorylated by two dihydroxyacetone kinases, DHAK I and DHAK II, which are ATP and PEP-dependent, respectively [8], and then channeled into glycolysis. In a coupled reductive pathway, glycerol is converted to 3-hydroxypropionaldehyde (3-HPA) by glycerol dehydratase (GDHt). The important intermediate is then reduced to 1,3-PD by the enzyme 1,3-propanediol oxydoreductase (PDOR) and hypothetical oxydoreductase (HOR) in the oxidation of reducing equivalent that is generated by the oxidative pathway [9–11].

Forage and Lin reported that GDHt, PDOR, GDH and DHAK I are coordinately expressed and are induced by glycerol or dihydroxyacetone [12]. Tong *et al.* showed that the genes for these four enzymes are organized as a cluster on the chromosome and called it the *dha* regulon [13]. Subsequently, DHAK II, the new

Received 2011-03-30, accepted 2011-07-01.

* Supported by the National High Technology Research and Development Program of China (2007AA02Z208) and the State Key Development Program for Basic Research of China (2007CB714304).

** To whom correspondence should be addressed. E-mail: zhixiu@dlut.edu.cn

enzyme, is first shown to be related to the *dha* regulon by the comparative genome analysis [8]. DHAK II includes the three soluble protein subunits that are encoded by the ORFs (open reading frame) *dhak1*, *dhak2* and *dhak3*. The expression of hypothetical oxidoreductase (HOR) is 89% identical to the hypothetical oxidoreductase of *E. coli* (*yqhD*) induced by 3-HPA accumulation [10]. It indicates that HOR does not belong to the *dha* regulon.

Many researchers have tried to use metabolic engineering to improve the production of 1,3-PD [14–16], but 1,3-PD production does not increase significantly compared to the wild strain. Furthermore, some mathematical models have been established to optimize and control the bioconversion of glycerol to 1,3-PD. The fermentation of glycerol by *K. pneumoniae* is a complex bioprocess because cell growth is subjected to multiple inhibitions by substrate and products. An excess kinetic model for substrate consumption and product formation has been proposed [17–20]. The model improved by Xiu *et al.* has become more feasible to describe substrate consumption and product formation in a large range of feed glycerol concentration in the medium [21]. Based on these studies, Sun *et al.* have supposed a structured model, which considers the intracellular components (*i.e.* 1,3-PD, glycerol and 3-HPA) and enzymes (such as GDHt and PDOR) [22]. Moreover, the inhibitory effect of 3-HPA on the activity of GDHt and PDOR is well characterized [22]. Zeng has proposed that a strong feedback inhibition and global regulations are involved in the expression of genes from the *dha* regulon [23]. However, the global regulation of gene expression is not yet clear.

In this study, we attempt to obtain more insights into the genetic regulation of the *dha* regulon by establishing a new model, which includes the expression of gene-mRNA-enzyme-product. The robustness of the model with respect to the biochemical system is examined. The influences of initial glycerol concentration and dilution rate on the biosynthesis of 1,3-PD and stability of the *dha* regulon model are also investigated. The results may further expand our understanding of the global regulation of genetic expression of the *dha* regulon.

2 MATHEMATICAL MODEL

The *dha* regulon is induced by dihydroxyacetone (DHA) in the absence of an exogenous acceptor as shown in Fig. 1 [2, 8, 10].

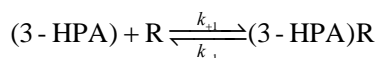
In the reductive pathway of glycerol metabolism, the toxic intermediate 3-HPA plays an important role and its accumulation would lead to lower rates of substrate consumption and 1,3-PD formation, eventually resulting in cessation of growth [10, 24]. The inhibitory effects of 3-HPA on the activity of GDH, GDHt and PDOR have been investigated [10, 22, 25]. Most of these researches focused on the effects of 3-HPA on the key enzymes of metabolism, cell growth, substrate consumption and target product formation. The previous

investigations also indicate that 3-HPA could be inhibitory to DNA synthesis because its aldehyde group may have a similar effect on DNA as that produced by formaldehyde [26, 27].

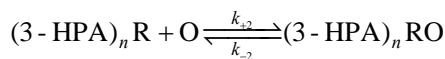
Based on these investigations, we postulate that 3-HPA accumulation represses the expression of *dha* regulon at the transcriptional level. A mathematical mode for the expression of gene-mRNA-enzyme-product is established to consider the repression of the *dha* regulon by 3-HPA, which is considered to occur in two steps as in the *trp* operon [28]. As a co-repressor, 3-HPA first binds to the repressor protein (*dhaR*) to form a holorepressor complex. This complex then binds specifically to the *dha* regulon and prevents the movement of RNA polymerase, and thereby blocks the transcription of the structural genes. Considering the complexity of the oxidative pathway and lack of experimental data, the oxidative pathway is conducted as a “black box” model.

2.1 Repression of *dha* regulon by 3-HPA

The repression may be considered as multiple-step equilibrium reactions according to the *trp* operon of *E. coli*: 3-HPA first binds to a free repressor (R) to form a product-repressor complex, (3-HPA)_nR (holorepressor). The repressor may have *n* binding sites. Subsequently, the holorepressor binds to an operator (O) to form a holorepressor-operator complex (3-HPA)_nRO. The first reaction is the limiting step while the other steps are rapid. Formation of the complex can be formulated as follows:



.....



$$K_d = \frac{k_{-1}}{k_{+1}} \quad K_0 = \frac{k_{-2}}{k_{+2}}$$

The concentrations of holorepressor and free operator at equilibrium can be derived according to the Scatchard equation as follows:

$$[(3\text{-HPA})_n\text{R}] = \frac{C_{3\text{-HPA}} \cdot R_t}{C_{3\text{-HPA}} + K_d} \quad (1)$$

$$[\text{O}] = \frac{[\text{O}_t](C_{3\text{-HPA}} + K_d)}{(C_{3\text{-HPA}} + K_d) + rC_{3\text{-HPA}}} \quad r = \frac{R_t}{K_0} \quad (2)$$

where [O], [O_t] and R_t are concentrations of free operator, total operator and repressor, respectively, [(3-HPA)_nR] is the concentration of holorepressor, *n* represents the binding sites, K_d and K₀ are the dissociation constants of holorepressor and holorepressor-operator, respectively.

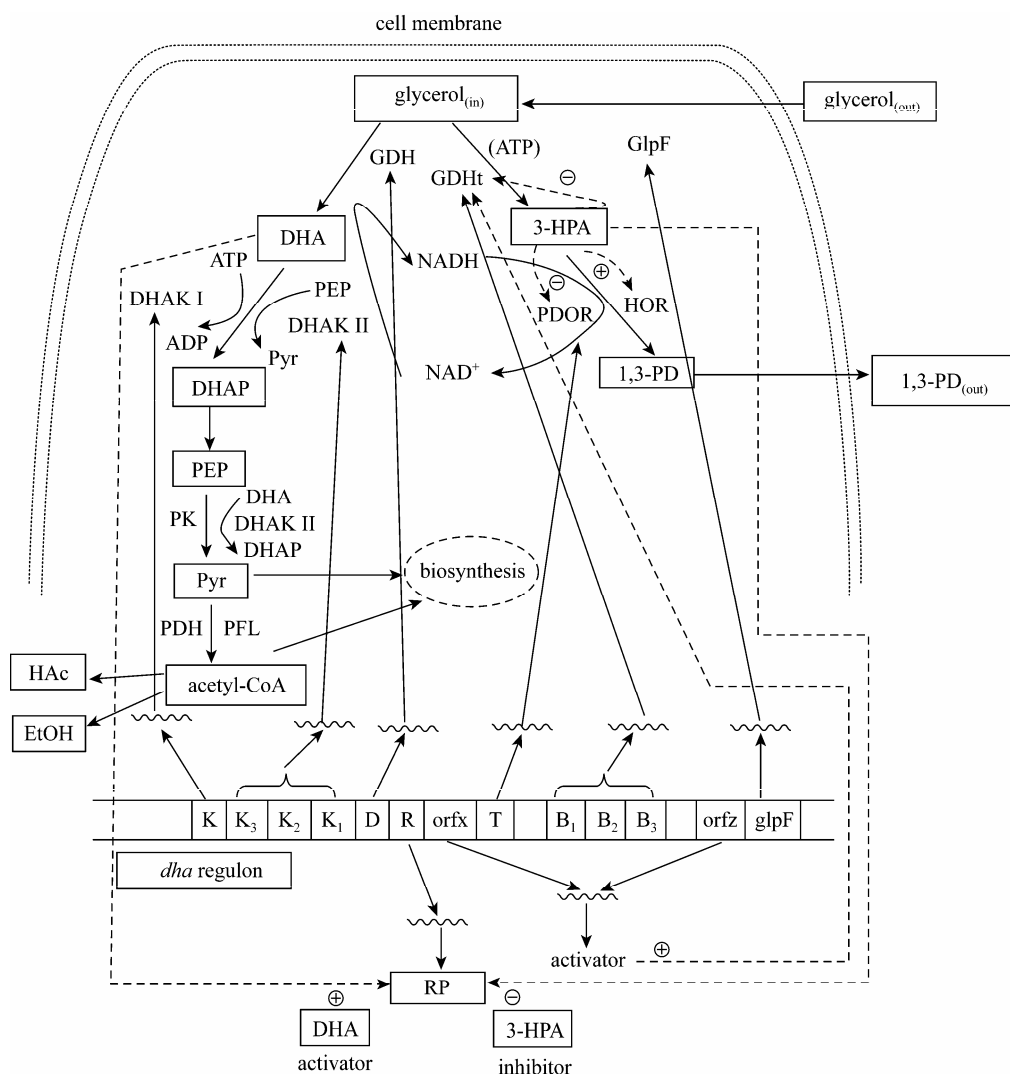


Figure 1 Main pathway of 1,3-propanediol biosynthesis in *K. pneumoniae*

(the regulatory and structural genes involved in the regulations of the *dha* regulon [2, 8, 10])

GDH—glycerol dehydrogenase; GDHt—glycerol dehydratase; DHAK I—dihydroxyacetone kinases (ATP dependent); DHAK II—dihydroxyacetone kinases (PEP dependent); PDOR—1,3-propanediol oxidoreductase; HOR—hypothetical oxidoreductase; PDH—pyruvate dehydrogenase; PFL—pyruvate format lyase; DHA—dihydroxyacetone; DHAP—dihydroxyacetone phosphate; PEP—phosphoenolpyruvate; Pyr—pyruvate; HAc—acetate; EtOH—ethanol; 3-HPA—3-hydroxypropionaldehyde; 1,3-PD—1,3-propanediol; RP—regulatory protein

2.2 Kinetics of repressor inhibited by 3-HPA

DhaR, encoded by gene *dhaR* in the *dha* regulon, shows a high degree of similarity to the AAA⁺ (AT-Pases associated with various cellular activities) family of enhancer binding proteins [27]. Previous investigations have indicated that *dhaR* is an activator for transcription factor, and it is induced by the expression of DHAK in *E. coli* and GDH in *C. freundii* [27, 29, 30]. Zheng *et al.* over-expressed the gene of *dhaR* from *Klebsiella pneumoniae* in a plasmid, resulting in increased expression of 1,3-propanediol oxidoreductase, indicating that *dhaR* acts as a positive regulator for gene *dhaT* [27]. Furthermore, GDHt and PDOR have

been over-expressed separately or together in *Klebsiella pneumoniae* to investigate their effects on glycerol fermentation. Unfortunately, the excessive expression of GDHt and PDOR is not favorable for increasing the production of 1,3-PD *via* glycerol fermentation by *K. pneumoniae*. Instead, this leads to serious impairment of cell growth and instability of plasmids, probably due to the accumulation of 3-HPA [27].

The equations governing the repressor are formulated as follows. This process consists of the transcription of *dhaR* to yield mRNA (M_R), followed by the translation of the mRNA to form the repressor (R):

$$\frac{dM_R}{dt} = K_{M_R} G_D [O] - (k_{M_R} + \mu) M_R \quad (3)$$

$$\frac{dR}{dt} = K_R M_R - (k_R + \mu)R - k_{-1}[(3\text{-HPA})_n R] \quad (4)$$

where M_R and R represent the concentrations of mRNA coding repressor and free repressor, respectively; G_D is the gene dosage; K_{M_R} and K_R are the rate constants for the formation of the species denoted by the subscripts; k_{M_R} and k_R are the degradation rates of M_R and R ; and μ is the specific growth rate of cells. The third term on the right-hand side of Eq. (4) denotes the decrease in repressor concentration caused by 3-HPA bound to the free repressor.

2.3 Kinetics of the two key enzymes GDHt and PDOR inhibited by 3-HPA

Transcription of the *dha* regulon yields mRNAs of GDHt and PDOR, which are then translated into the corresponding enzymes (GDHt and PDOR). We postulate that the formation of mRNAs and enzymes belongs to the first order kinetics. The degradations of mRNAs and enzymes and the dilution effect due to cell growth are considered. The equations governing the levels of mRNAs and protein synthesis for GDHt and PDOR are formulated as follows:

$$\frac{dM_{\text{GDHt}}}{dt} = K_m^{\text{GDHt}} G_D [\text{O}_1] - (k_d^{\text{mGDHt}} + \mu) M_{\text{GDHt}} \quad (5)$$

$$\frac{dM_{\text{PDOR}}}{dt} = K_m^{\text{PDOR}} G_D [\text{O}_1] - (k_d^{\text{mPDOR}} + \mu) M_{\text{PDOR}} \quad (6)$$

$$\frac{d[\text{GDHt}]}{dt} = K_{\text{GDHt}} M_{\text{GDHt}} - (k_d^{\text{GDHt}} + \mu)[\text{GDHt}] \quad (7)$$

$$\frac{d[\text{PDOR}]}{dt} = K_{\text{PDOR}} M_{\text{PDOR}} - (k_d^{\text{PDOR}} + \mu)[\text{PDOR}] \quad (8)$$

where M_{GDHt} and M_{PDOR} are the mRNA concentrations denoted by the subscripts; $[\text{GDHt}]$ and $[\text{PDOR}]$ represent the enzyme concentrations of GDHt and PDOR, respectively; K_m^{GDHt} and K_m^{PDOR} are the rate constants for the formation of GDHt mRNA and PDOR mRNA, respectively, whereas K_{GDHt} and K_{PDOR} are the rate constants for formation of GDHt and PDOR, respectively; k_d^{mGDHt} and k_d^{mPDOR} represent the rate constants for the degradation of GDHt mRNA and PDOR mRNA, respectively, and k_d^{GDHt} and k_d^{PDOR} represent the rate constants for the degradation of GDHt and PDOR, respectively.

For convenience, by defining

$$m_{\text{GDHt}} = \frac{M_{\text{GDHt}}}{K_m^{\text{GDHt}} \cdot G_D \cdot [\text{O}_1]};$$

$$K_{\text{GDHt}}^m = K_m^{\text{GDHt}} \cdot K_{\text{GDHt}} \cdot G_D \cdot [\text{O}_1];$$

$$m_{\text{PDOR}} = \frac{M_{\text{PDOR}}}{K_m^{\text{PDOR}} \cdot G_D \cdot [\text{O}_1]};$$

$$K_{\text{PDOR}}^m = K_m^{\text{PDOR}} \cdot K_{\text{PDOR}} \cdot G_D \cdot [\text{O}_1];$$

$$m_R = \frac{M_R}{K_{M_R} \cdot G_D \cdot [\text{O}_1]}; \quad K_\theta = K_R K_{M_R} G_D [\text{O}_1]$$

we rewrite Eqs. (3)–(8) in the following form

$$\frac{dm_{\text{GDHt}}}{dt} = \frac{C_{3\text{-HPA}} + K_d}{(C_{3\text{-HPA}} + K_d) + rC_{3\text{-HPA}}} - (k_d^{\text{mGDHt}} + \mu) m_{\text{GDHt}}$$

$$\frac{d[\text{GDHt}]}{dt} = K_{\text{GDHt}}^m \cdot m_{\text{GDHt}} - (k_d^{\text{GDHt}} + \mu)[\text{GDHt}]$$

$$\frac{dm_{\text{PDOR}}}{dt} = \frac{C_{3\text{-HPA}} + K_d}{(C_{3\text{-HPA}} + K_d) + rC_{3\text{-HPA}}} - (k_d^{\text{mPDOR}} + \mu) m_{\text{PDOR}}$$

$$\frac{d[\text{PDOR}]}{dt} = K_{\text{PDOR}}^m \cdot m_{\text{PDOR}} - (k_d^{\text{PDOR}} + \mu)[\text{PDOR}]$$

$$\frac{dm_R}{dt} = \frac{C_{3\text{-HPA}} + K_d}{(C_{3\text{-HPA}} + K_d) + rC_{3\text{-HPA}}} - (k_{M_R} + \mu) m_R$$

$$\frac{dR}{dt} = K_\theta m_R - (k_R + \mu)R - k_{-1}[(3\text{-HPA})_n R] \quad (9)$$

2.4 Total kinetic model of *dha* regulon repressed by 3-HPA

In our previous work [22], a mathematical model was set up to describe the continuous and batch fermentations of glycerol by *K. pneumoniae*. The enzyme-catalytic kinetics on the reductive pathway, the transport of glycerol and diffusion of 1,3-PD across cell membrane, and the inhibition of GDHt and PDOR by 3-HPA were well investigated. The model can be used to describe the consumption rate of substrate and the formation rates of biomass and main products. The intracellular concentrations of glycerol, 1,3-PD and 3-HPA can be predicted for continuous and batch cultures. The analysis indicated that 3-HPA inhibits the activity of PDOR more than that of GDHt. Based on our previous investigation, a new mathematical model involving gene regulation for the *dha* regulon and enzyme catabolism of glycerol bioconversion is obtained.

$$\frac{dm_R}{dt} = \frac{C_{3\text{-HPA}} + K_d}{(C_{3\text{-HPA}} + K_d) + rC_{3\text{-HPA}}} - (k_{M_R} + \mu) m_R \quad (10)$$

$$\frac{dR}{dt} = K_\theta m_R - (k_R + \mu)R - k_{-1}[(3\text{-HPA})_n R] \quad (11)$$

$$\frac{dm_{\text{GDHt}}}{dt} = \frac{C_{3\text{-HPA}} + K_d}{(C_{3\text{-HPA}} + K_d) + rC_{3\text{-HPA}}} - (k_d^{\text{mGDHt}} + \mu) m_{\text{GDHt}} \quad (12)$$

$$\frac{d[\text{GDHt}]}{dt} = K_{\text{GDHt}}^m \cdot m_{\text{GDHt}} - (k_d^{\text{GDHt}} + \mu)[\text{GDHt}] \quad (13)$$

$$\frac{dm_{\text{PDOR}}}{dt} = \frac{C_{3\text{-HPA}} + K_d}{(C_{3\text{-HPA}} + K_d) + rC_{3\text{-HPA}}} - (k_d^{\text{mPDOR}} + \mu)m_{\text{PDOR}} \quad (14)$$

$$\frac{d[\text{PDOR}]}{dt} = K_{\text{PDOR}}^m \cdot m_{\text{PDOR}} - (k_d^{\text{PDOR}} + \mu)[\text{PDOR}] \quad (15)$$

$$\frac{dX}{dt} = X(\mu - D) \quad (16)$$

$$\frac{dC_{\text{se}}}{dt} = D(C_{\text{so}} - C_{\text{se}}) - q_s X \quad (17)$$

$$\frac{dC_{\text{si}}}{dt} = \frac{1}{V_s} \left[J_{\text{max}} \frac{C_{\text{se}}}{C_{\text{se}} + K_m} + \frac{1}{A_s} (C_{\text{se}} - C_{\text{si}}) - q_s \right] - \mu C_{\text{si}} \quad (18)$$

$$A_s = \frac{\delta}{B \times D_f}$$

$$\frac{dC_{3\text{-HPA}}}{dt} = k_1[\text{GDHt}] \frac{C_{\text{si}}}{K_{\text{mGDHt}} \left(1 + \frac{C_{3\text{-HPA}}}{K_1^{\text{GDHt}}} \right) + C_{\text{si}}} - k_2[\text{PDOR}] \frac{C_{3\text{-HPA}}}{K_{\text{mPDOR}} + C_{3\text{-HPA}} \left(1 + \frac{C_{3\text{-HPA}}}{K_1^{\text{PDOR}}} \right)} - \mu C_{3\text{-HPA}} - nk_{-1}[(3\text{-HPA})_n \text{R}] \quad (19)$$

$$\frac{dC_{\text{PDi}}}{dt} = k_2[\text{PDOR}] \frac{C_{3\text{-HPA}}}{K_{\text{mPDOR}} + C_{3\text{-HPA}} \left(1 + \frac{C_{3\text{-HPA}}}{K_1^{\text{PDOR}}} \right)} - K_{\text{PD}}(C_{\text{PDi}} - C_{\text{PDe}}) - \mu C_{\text{PDi}} \quad (20)$$

$$\frac{dC_{\text{PDe}}}{dt} = q_{\text{PDe}} X - DC_{\text{PDe}} \quad (21)$$

$$\frac{dC_{\text{HAc}}}{dt} = q_{\text{HAc}} X - DC_{\text{HAc}} \quad (22)$$

$$\frac{dC_{\text{EtOH}}}{dt} = q_{\text{EtOH}} X - DC_{\text{EtOH}} \quad (23)$$

$$\mu = \mu_m \frac{C_{\text{se}}}{C_{\text{se}} + K_s} \left(1 - \frac{C_{\text{se}}}{C_{\text{se}}^*} \right) \left(1 - \frac{C_{\text{PDe}}}{C_{\text{PDe}}^*} \right) \times \left(1 - \frac{C_{\text{EtOH}}}{C_{\text{EtOH}}^*} \right) \left(1 - \frac{C_{\text{HAc}}}{C_{\text{HAc}}^*} \right) \quad (24)$$

$$q_s = m_s + \frac{\mu}{Y_s^m} + \Delta q_s^m \frac{C_{\text{se}}}{C_{\text{se}} + K_s^*} \quad (25)$$

$$q_{pi} = m_{pi} + \frac{\mu}{Y_{pi}^m} + \Delta q_{pi}^m \frac{C_{\text{se}}}{C_{\text{se}} + K_{pi}^*} \quad (26)$$

(pi = 1, 3 - PD, HAc, EtOH)

Equation (19) describes the change of intracellular 3-HPA concentration as a function of time. The first and second terms on the right-hand side of Eq. (19) express the production of 3-HPA catalyzed by GDHt and consumption of 3-HPA catalyzed by PDOR, respectively. Inhibition of GDHt and PDOR activities by 3-HPA is also considered. The third term represents the dilution effect on the intracellular concentration of 3-HPA. The last term indicates the demand of 3-HPA bound to the aporepressor. Other equations have been investigated in previous work [18–22]. The kinetic parameters chosen from the literature for Eqs. (10)–(26) are listed in Table 1.

2.5 Methods of simulation

The kinetic parameters in Eqs. (10)–(26) are determined by the method of multidimensional constrained nonlinear minimization supplied in the software MATLAB based on 58 groups of experimental data [18–21, 31].

The techniques of multiplicity simulation are developed from the software Mathematica. For continuous fermentation, the steady state solutions is obtained at a given set of concentration and dilution rate for the feed substrate by substituting the left hand sides of Eqs. (10)–(23) with zero. Gröbner Basis method supplied in the software Mathematica is used.

3 RESULTS AND DISCUSSION

3.1 Determination of parameters in Eqs. (10)–(26)

The kinetic parameters in Eqs. (10)–(26) are determined by comparing the computational values with the reported experimental extracellular concentrations of 1,3-PD [18–21, 31]. The average relative error of the computational values to the experimental extracellular concentrations of 1,3-PD is chosen as an objective function. The average relative error is 11.75% as shown in Fig. 2.

3.2 Translation of original model to S-system and analysis of robustness

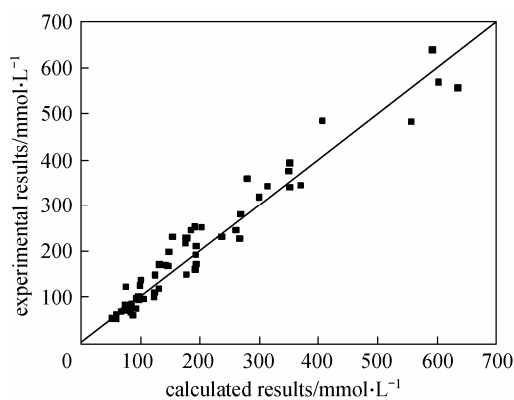
S-system model is set up according to the proposed mathematical model [33, 34]. The robustness analysis is developed according to the S-system. The transition from the mathematical model to the numerical S-system model requires the determination of 28 rate

Table 1 Kinetic parameters for Eqs. (10)–(26) associated with the *dha* regulon and 1,3-PD biosynthesis in *K. pneumoniae*

Parameters	Reported value	References	Parameters	Reported value	References
V_s	0.151 L·g ⁻¹	[22]	Y_s^m	0.0082 g·mmol ⁻¹	[21]
J_{\max}	54.664 mmol·g ⁻¹ ·h ⁻¹	[22]	$Y_{1,3-PD}^m$	67.69 g·mmol ⁻¹	[21]
K_m	1.340 mmol·L ⁻¹	[22]	Y_{HAc}^m	33.07 g·mmol ⁻¹	[21]
A_s	1.896×10 ⁻⁴ g·L ⁻¹ ·h ⁻¹	[22]	Y_{EtOH}^m	11.66 g·mmol ⁻¹	[21]
K_i^{GDHt}	220.319 mmol·L ⁻¹	[22]	Δq_s^m	28.58 mmol·g ⁻¹ ·h ⁻¹	[21]
K_i^{PDOR}	0.418 mmol·L ⁻¹	[22]	$\Delta q_{1,3-PD}^m$	26.59 mmol·g ⁻¹ ·h ⁻¹	[21]
K_{PD}	25.177 h ⁻¹	[22]	Δq_{HAc}^m	5.74 mmol·g ⁻¹ ·h ⁻¹	[21]
m_s	2.20 mmol·g ⁻¹ ·h ⁻¹	[21]	Δq_{EtOH}^m	—	[21]
$m_{1,3-PD}$	-2.69 mmol·g ⁻¹ ·h ⁻¹	[21]	K_s^*	11.4 3mmol·L ⁻¹	[21]
m_{HAc}	-0.97 mmol·g ⁻¹ ·h ⁻¹	[21]	$K_{1,3-PD}^*$	15.50 mmol·L ⁻¹	[21]
m_{EtOH}	5.26 mmol·g ⁻¹ ·h ⁻¹	[21]	K_{HAc}^*	85.71 mmol·L ⁻¹	[21]
μ_m	0.67 h ⁻¹	[32]	K_{EtOH}^*	—	[21]
K_s	0.28 mmol·L ⁻¹	[32]	C_{se}^*	2039 mmol·L ⁻¹	[32]
$C_{1,3-PD}^*$	939.5 mmol·L ⁻¹	[32]	C_{HAc}^*	1026 mmol·L ⁻¹	[32]
C_{EtOH}^*	360.9 mmol·L ⁻¹	[32]			

Table 2 Computational results of the parameters in Eqs. (10)–(26)

$K_d/\text{mmol}\cdot\text{L}^{-1}$	k_R/h^{-1}	k_{M_R}/h^{-1}	k_d^{GDHt}/h^{-1}	$K_\theta/\text{mmol}\cdot\text{L}^{-1}\cdot\text{h}^{-2}$	k_{-1}/h^{-1}	k_1/h^{-1}	n
917.9722	1.1305×10 ⁵	0.1096	12.7837	0.2004	79.9150	36.3625	2.0421
$k_d^{mGDHt}/\text{h}^{-1}$	$k_d^{mPDOR}/\text{h}^{-1}$	K_{GDHt}^m/h^{-1}	K_{PDOR}^m/h^{-1}	$R_v/\text{mmol}\cdot\text{L}^{-1}$	k_d^{PDOR}/h^{-1}	k_2/h^{-1}	r
1.5462	11.4334	10.8083	24.1030	1.48×10 ⁻⁵	20.2310	42.5261	13.1567

**Figure 2** Comparison between experimental and calculated concentrations for 1,3-PD

constants (14 p_i and 14 q_i), as well as 134 kinetic orders (58 $g_{i,j}$ and 76 $h_{i,j}$) under the steady state of dilution rate of 0.1 h⁻¹ and initial glycerol concentration of 164 mmol·L⁻¹. The values of these parameters are estimated by the method reported in literature [33, 34].

$$\frac{dX}{dt} = 3.5558 C_{se}^{0.7943} C_{PDe}^{-0.0530} C_{HAc}^{-0.0263} C_{EtOH}^{-0.2747} X - DX$$

$$\frac{dC_{se}}{dt} = DC_{so} - 299.129 D^{0.00044} X^{0.9996} C_{se}^{0.6771} \times$$

$$C_{PDe}^{-0.0443} C_{HAc}^{-0.0220} C_{EtOH}^{-0.2297}$$

$$\frac{dC_{PDe}}{dt} = 1428.53 C_{se}^{1.3087} C_{PDe}^{-0.0853} C_{HAc}^{-0.0424} \times$$

$$C_{EtOH}^{-0.4424} X - DC_{PDe}$$

$$\frac{dC_{HAc}}{dt} = 364.785 C_{se}^{1.1238} C_{PDe}^{-0.0748} C_{HAc}^{-0.0372} \times$$

$$C_{EtOH}^{-0.3879} X - DC_{HAc}$$

$$\frac{dC_{EtOH}}{dt} = 83.97 C_{se}^{0.5253} C_{PDe}^{-0.0399} C_{HAc}^{-0.0198} \times$$

$$C_{EtOH}^{-0.2066} X - DC_{EtOH}$$

$$\frac{dm_R}{dt} = 0.6322 K_d^{0.1787} r^{-0.1818} C_{3-HPA}^{-0.1787} -$$

$$3.6592 k_{m_R}^{0.5230} C_{se}^{0.3789} m_R C_{PDe}^{-0.0253} C_{HAc}^{-0.0126} C_{EtOH}^{-0.1310}$$

$$\frac{dR}{dt} = K_\theta m_R - 1.0003 k_R^{0.9999} k_{-1}^{2.5531 \times 10^{-5}} R_t^{2.5531 \times 10^{-5}} \times$$

$$C_{se}^{7.0262 \times 10^{-7}} R^{0.9999} C_{3-HPA}^{2.51 \times 10^{-5}} K_d^{-2.51 \times 10^{-5}} C_{PDe}^{-4.6860 \times 10^{-8}} \times$$

$$C_{HAc}^{-2.3305 \times 10^{-8}} C_{EtOH}^{-2.4297 \times 10^{-7}}$$

$$\begin{aligned}
\frac{dm_{\text{GDHt}}}{dt} &= 0.6322K_d^{0.1787}r^{-0.1818}C_{3\text{-HPA}}^{-0.1787} - \\
&\quad 1.3581k_d^{\text{mGDHt}0.9393}C_{\text{se}}^{0.0483}m_{\text{GDHt}}C_{\text{PDe}}^{-0.0032} \times \\
&\quad C_{\text{HAc}}^{-0.0016}C_{\text{EtOH}}^{-0.0167} \\
\frac{dm_{\text{PDOR}}}{dt} &= 0.6322K_d^{0.1787}r^{-0.1818}C_{3\text{-HPA}}^{-0.1787} - \\
&\quad 1.0627k_d^{\text{mPDOR}0.9913}C_{\text{se}}^{0.0069}m_{\text{PDOR}} \times \\
&\quad C_{\text{PDe}}^{-4.5934 \times 10^{-4}}C_{\text{HAc}}^{-2.2844 \times 10^{-4}}C_{\text{EtOH}}^{-0.0024} \\
\frac{d[\text{GDHt}]}{dt} &= K_{\text{GDHt}}^m m_{\text{GDHt}} - 1.0569k_d^{\text{GDHt}0.9922} \times \\
&\quad C_{\text{se}}^{0.0062}[\text{GDHt}]C_{\text{PDe}}^{-4.1120 \times 10^{-4}} \times \\
&\quad C_{\text{HAc}}^{-2.0451 \times 10^{-4}}C_{\text{EtOH}}^{-0.0021} \\
\frac{d[\text{PDOR}]}{dt} &= K_{\text{PDOR}}^m m_{\text{PDOR}} - 1.0380k_d^{\text{PDOR}0.9951} \times \\
&\quad C_{\text{se}}^{0.0039}[\text{PDOR}]C_{\text{PDe}}^{-2.6058 \times 10^{-4}} \times \\
&\quad C_{\text{HAc}}^{-1.2959 \times 10^{-4}}C_{\text{EtOH}}^{-0.0014} \\
\frac{dC_{3\text{-HPA}}}{dt} &= 0.5684K_i^{\text{GDHt}0.0594}k_1C_{\text{si}}^{0.8899}K_m^{\text{GDHt}-0.8899} \times \\
&\quad C_{3\text{-HPA}}^{-0.0594}[\text{GDHt}] - 4.0788K_i^{\text{PDOR}0.0539} \times \\
&\quad k_{-1}^{2.4434 \times 10^{-5}}R_t^{2.4434 \times 10^{-5}}k_2^{0.0553}n^{2.4434 \times 10^{-5}} \times \\
&\quad C_{\text{se}}^{0.7504}[\text{PDOR}]^{0.0553}C_{3\text{-HPA}}^{0.8908}K_{\text{mPDOR}}^{-1.2691 \times 10^{-5}} \times \\
&\quad K_d^{-2.4022 \times 10^{-5}}C_{\text{PDe}}^{-0.05}C_{\text{HAc}}^{-0.0249}C_{\text{EtOH}}^{-0.2595} \\
\frac{dC_{\text{si}}}{dt} &= 1.0425J_{\text{max}}^{0.0073}C_{\text{se}}^{0.9996}V_s^{-1}K_m^{-0.0069}A_s^{-0.9927} - \\
&\quad 1.4577C_{\text{se}}^{-0.0256}C_{\text{si}}^{0.9621}V_s^{-0.9999}A_s^{-0.9621} \times \\
&\quad C_{\text{PDe}}^{-0.0017}C_{\text{HAc}}^{-0.0008}C_{\text{EtOH}}^{-0.0087} \\
\frac{dC_{\text{PDi}}}{dt} &= 1.0008K_{\text{PD}}^{0.9999}K_i^{\text{PDOR}7.5703 \times 10^{-5}}k_2^{7.7729 \times 10^{-5}} \times \\
&\quad C_{\text{PDe}}^{0.9999}[\text{PDOR}]^{7.7729 \times 10^{-5}}K_m^{\text{PDOR}(-1.7824 \times 10^{-8})} \times \\
&\quad C_{3\text{-HPA}}^{-7.5686 \times 10^{-5}} - 1.0314K_{\text{PD}}^{0.9960}C_{\text{se}}^{0.0031}C_{\text{PDi}} \times \\
&\quad C_{\text{PDe}}^{-2.0992 \times 10^{-4}}C_{\text{HAc}}^{-1.044 \times 10^{-4}}C_{\text{EtOH}}^{-0.0011}
\end{aligned} \tag{27}$$

Local stability is confirmed by examining the eigenvalues of the local representation of the system at its steady state. The real parts of all eigenvalues are negative, indicating that the nominal steady state is locally stable and that the system would return to this steady state following small perturbations.

Robustness describes how deeply the system would suffer as a result of small perturbations. Rate constant sensitivities are the influences of small changes in rate constants on the metabolites and fluxes of system. The sensitivities for metabolite concentrations are

presented in Fig. 3 (a). Of the total 98 rate constant sensitivities, 86 (87.8%) have values below 1, implying that the response to a perturbation in a rate constant would be attenuated in most parts of the system. 12 (12.2%) have values higher than 1, indicating that parameter change has little influence on the S-system model.

Kinetic order sensitivities are the influences of small changes in kinetic order parameters on metabolites and fluxes of system. The influence of the kinetic orders on the concentrations of metabolites is shown in Fig. 3 (b). The analysis indicates that of the 1876 kinetic order sensitivities, 1758 (93.7%) are below 1, 116 (6.2%) are between 1 and 10, and only 2 (0.1%) are a little larger than 10.

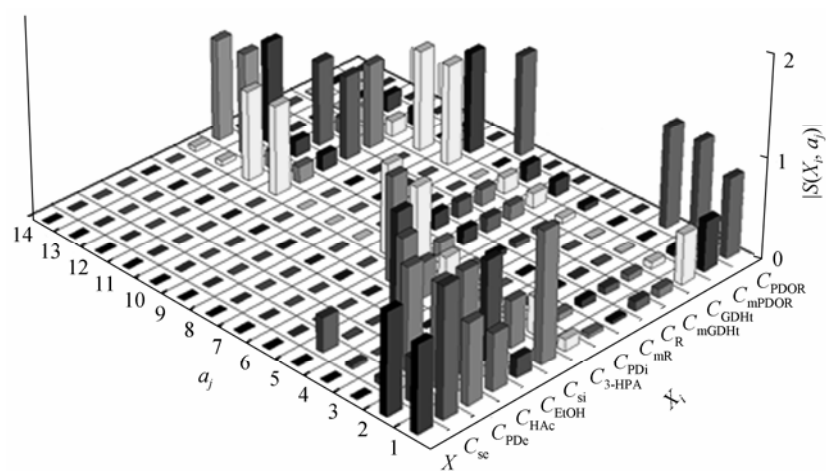
Effects of alterations on independent variables are quantified by logarithmic gains. Logarithmic gains with respect to metabolite concentrations are depicted in Fig. 3 (c). Of the 350 logarithmic gains, 341 (97.4%) are below 1 and 9 (2.6%) are little larger than 1. Large influences occur for dilution rate (D) and initial glycerol concentration (C_{so}) on the intracellular concentration of 1,3-propanediol. Therefore, the two variables may be good candidates for manipulating and optimizing the production of 1,3-PD.

The influences of small changes in the parameters listed in Table 2 on metabolite concentrations of the system are also presented in Fig. 3 (c). Of the total 224 parameters sensitivities, 219 (97.8%) are below 1 and 5 (2.2%) are a little higher than 1, indicating that changes in parameters have little influence on the S-system model and the parameters selected in Table 2 are reasonable.

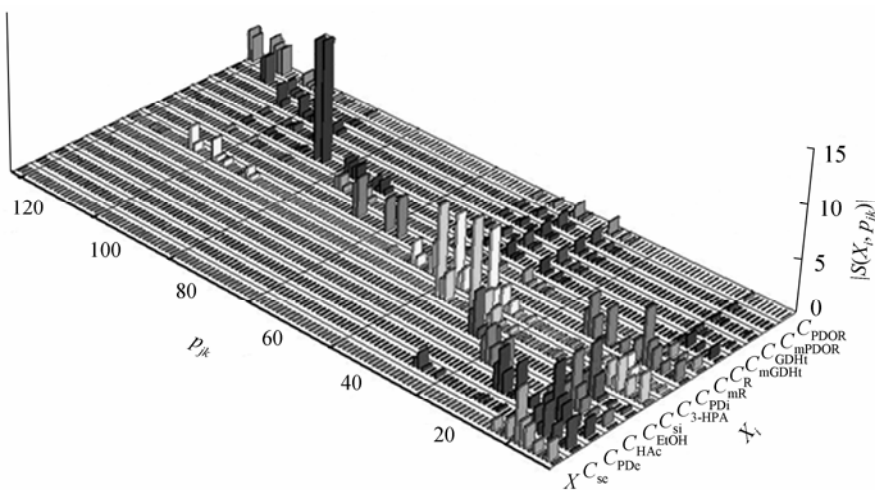
3.3 Simulation of continuous cultures and multiplicity analysis

Figure 4 shows the steady state of biomass, concentrations of extracellular residual glycerol, extracellular 1,3-PD, acetate, and ethanol as a function of substrate concentration (C_{so}) in the feed medium at constant dilution rate ($D = 0.1 \text{ h}^{-1}$). The multiplicity appears between two regions. One is between $C_{\text{so}} = 1144 \text{ mmol}\cdot\text{L}^{-1}$ and $1274 \text{ mmol}\cdot\text{L}^{-1}$, in which there exist three steady-state solutions of the system equations. Another multiplicity with two steady-state solutions appears between $C_{\text{so}} = 1735 \text{ mmol}\cdot\text{L}^{-1}$ and $1986 \text{ mmol}\cdot\text{L}^{-1}$. Initial glycerol concentration over $1735 \text{ mmol}\cdot\text{L}^{-1}$ indicates that growth inhibition by excessive substrate is obvious and not benefit for 1,3-PD formation in actual production.

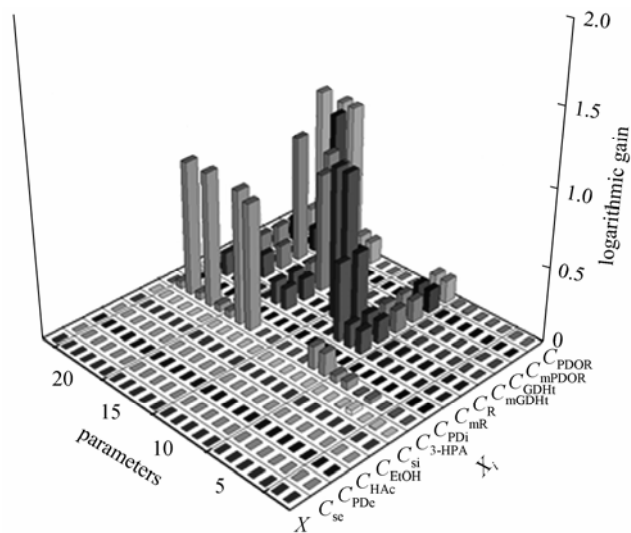
It was reported that the fermentation of glycerol by *K. pneumoniae* was a complex bioprocess since the microbial growth was subjected to multiple inhibitions of substrate and products, e.g. glycerol, acetate, ethanol and 1,3-PD [32]. Under substrate-excess conditions, the kinetics of substrate consumption and product formation behaved metabolic overflow. The metabolic overflow of product and its inhibition on cell growth led to nonlinear phenomena [18, 20, 31, 35-37]. In addition,



(a) Sensitivities of metabolite concentrations with respect to changes in rate constants



(b) Sensitivities of metabolite concentrations with respect to changes in kinetic orders



(c) Logarithmic gains of metabolites with respect to changes in independent variables

Figure 3 Robustness analysis of the *dha*-regulon model

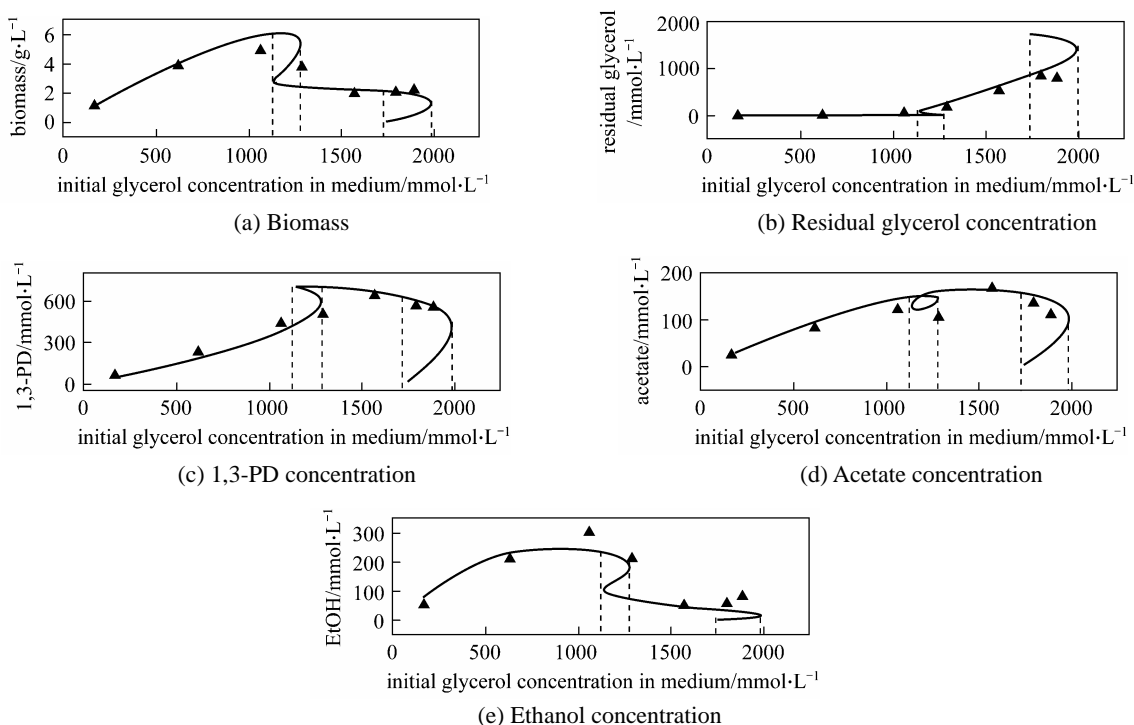


Figure 4 Comparison of biomass, substrate and product concentrations between experimental and simulated results at $D = 0.1 \text{ h}^{-1}$ but varied substrate feed concentrations in continuous cultures

▲ experimental; — simulation

the metabolic overflow could lead to high concentration and productivity of product. However, the concentration of residual glycerol during fermentation process must be high under this condition, which raises considerable problem in the separation process because of similar physical and chemical properties of glycerol and 1,3-PD [38]. Xiu *et al.* discussed the multiplicity and stability of a three-dimensional dynamic system [36]. Analysis showed that the combined effects of product inhibition and enhanced formation rate of product under excessive substrate concentrations caused the multiplicity and hysteresis. However, growth inhibition by substrate and enhanced substrate uptake appeared not to be necessary conditions to multiplicity formation. Based on Xiu *et al.*'s research [36], time delay was introduced to this system and Hopf bifurcation was obtained [39]. Subsequently, the existence of equilibrium points of five-dimensional nonlinear dynamic system was examined, which indicated the upper boundary of dilution rate decreased as substrate concentration in feed increased [40]. The inhibition potentials of substrate and products on the growth of *Clostridium butyricum* were also well investigated [32]. Subsequently, growth inhibition of *Clostridium butyricum* VPI 3266 by raw glycerol, obtained from the biodiesel production process, was examined. The strain presented the same tolerance to raw and to commercial glycerol under similar grade [7]. Under continuous culture, increase of inlet glycerol concentration resulted in somehow decreased biomass yield at steady-state conditions [5].

The experimental results of biomass, substrate and main products under continuous cultures at different initial glycerol concentrations and dilution rate of 0.1 h^{-1} by *K. pneumonia* are also depicted in Fig. 4. The simulation of microbial growth, substrate consumption and main product formation fit well with experimental results according to our fourteen-dimensional dynamic system. It was reported that *K. pneumoniae* was able to produce about 460–638 $\text{mmol}\cdot\text{L}^{-1}$ of 1,3-PD under continuous culture at dilution rates between 0.1 and 0.25 h^{-1} . In most of the cases, the observed molar yield of 1,3-PD to glycerol was between 0.35 and $0.65 \text{ mol}\cdot\text{mol}^{-1}$ [9, 41, 42]. According to previous stoichiometric analysis, the maximum theoretical yield of 1,3-PD from glycerol was $0.85 \text{ mol}\cdot\text{mol}^{-1}$ under micro-aerobic conditions and $0.72 \text{ mol}\cdot\text{mol}^{-1}$ under anaerobic conditions [43]. Moreover, in order to further reduce production cost, crude glycerol, as principal by-product from fat saponification, alcoholic beverage manufacture and biodiesel production units, are used for microbial production of 1,3-PD in industry [4, 5]. In fed-batch cultures of *K. pneumoniae*, the final 1,3-PD concentration ($697 \text{ mmol}\cdot\text{L}^{-1}$) obtained with glycerol derived from lipase-catalyzed methanolysis of soybean oil is comparable to that obtained with crude glycerol from alkali-catalyzed process ($675 \text{ mmol}\cdot\text{L}^{-1}$) [4]. The effect of inlet glycerol concentration and dilution rate on growth and 1,3-PD production by *C. butyricum* strains was investigated using raw glycerol as a substrate [7, 44]. At dilution rate of 0.3 h^{-1} , about $394 \text{ mmol}\cdot\text{L}^{-1}$ of

1,3-PD from $652 \text{ mmol}\cdot\text{L}^{-1}$ of feed glycerol was obtained under continuous culture. Significantly high 1,3-PD concentrations about $580\text{--}640 \text{ mmol}\cdot\text{L}^{-1}$ was achieved at low dilution rates according to other studies [5, 44]. In contrast, González-Pajuelo *et al.* reported that 1,3-PD yield (around $0.65 \text{ mol}\cdot\text{mol}^{-1}$) remained practically constant irrespective of feed substrate concentration or dilution rate [7].

The volumetric productivities of 1,3-PD at various dilution rates and initial glycerol concentrations in continuous cultures are shown in Fig. 5. Robustness analysis in Section 3.2 indicates dilution rate (D) and initial glycerol concentration (C_{s0}) may be good candidates as manipulating and optimizing variables for 1,3-PD production. For continuous fermentation by *K. pneumoniae*, optimum glycerol concentration and dilution rate were $731 \text{ mmol}\cdot\text{L}^{-1}$ and 0.29 h^{-1} , respectively. The corresponding productivity was $114 \text{ mmol}\cdot\text{L}^{-1}\cdot\text{h}^{-1}$ [38]. The maximum 1,3-propanediol volumetric productivity could be obtained at about $72.4 \text{ mmol}\cdot\text{L}^{-1}\cdot\text{h}^{-1}$ when a dilution rate of 0.29 h^{-1} and a feed glycerol concentration of $978 \text{ mmol}\cdot\text{L}^{-1}$ were used for *C. butyricum* strains [44]. The highest reported value of 1,3-PD volumetric productivity, $135.5 \text{ mmol}\cdot\text{L}^{-1}\cdot\text{h}^{-1}$, was achieved at dilution rate of 0.30 h^{-1} and feed glycerol concentration of $652 \text{ mmol}\cdot\text{L}^{-1}$ using *C. butyricum* VPI 3266 strain [45].

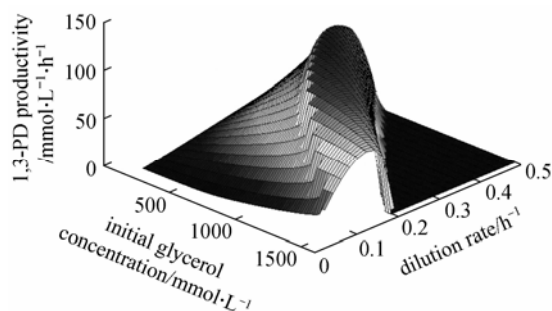


Figure 5 Volumetric productivities of 1,3-PD at various dilution rates and initial glycerol concentrations for continuous cultures

Figures 6–8 show the computational results for intracellular residual glycerol, 3-HPA and 1,3-PD concentrations at different initial glycerol concentrations and dilution rates in continuous cultures with *K. pneumoniae* as the fermenting bacteria. Intracellular residual glycerol concentration remains very low when the initial glycerol concentration is less than $1100 \text{ mmol}\cdot\text{L}^{-1}$ at fixed dilution rate of 0.1 h^{-1} , but will increase as the initial glycerol concentration increases. When the dilution rate is increased, residual glycerol concentration increases obviously since the fixed initial glycerol concentration is not benefit to 1,3-PD production. Intracellular 1,3-PD concentration initially increases but tends to decrease with the increases of feed glycerol concentration at a fixed dilution rate, while intracellular 3-HPA concentration increases rapidly with initial glycerol concentration and

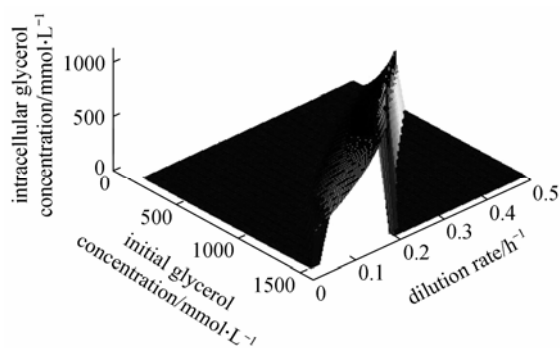


Figure 6 Computational results of intracellular residual glycerol concentrations at various dilution rates and initial glycerol concentrations for continuous cultures of *K. pneumoniae*

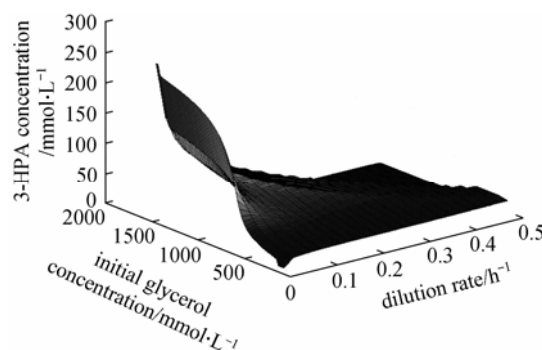


Figure 7 Computational results of intracellular 3-HPA concentrations at various dilution rates and initial glycerol concentrations for continuous cultures of *K. pneumoniae*

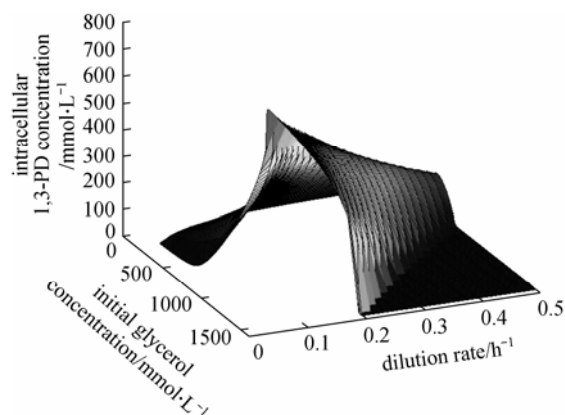


Figure 8 Computational results of intracellular 1,3-PD concentrations at various dilution rates and initial glycerol concentrations for continuous cultures of *K. pneumoniae*

then appears constant when the initial glycerol concentration reaches some values at a fixed dilution rate. The above results are in accordance with the previous research [22]. The accumulation of 3-HPA during the fermentation of glycerol to 1,3-PD was first demonstrated for *E. agglomerans* at high initial glycerol concentration [25]. It was reported that the final 3-HPA concentration could reach $30 \text{ mmol}\cdot\text{L}^{-1}$ at an initial glycerol concentration up to $725 \text{ mmol}\cdot\text{L}^{-1}$ when

3-HPA was added during the exponential growth phase of batch cultures. The lower the pH, the earlier 3-HPA accumulated [24, 25]. Moreover, at dilution rate of 0.30 h^{-1} and feed glycerol concentration of $60 \text{ g}\cdot\text{L}^{-1}$, 3-HPA accumulation was observed for the first time in the broth of *C. butyricum* culture [46]. According to previous models that consider the enzyme-catalyzed reductive pathway only, 3-HPA could accumulate during the fermentation process to a maximum concentration of $275 \text{ mmol}\cdot\text{L}^{-1}$ at dilution rate of 0.1 h^{-1} [22]. However, in our present models in which two regulated negative-feedback mechanisms of repression and enzyme inhibition are incorporated, 3-HPA accumulation is reduced to a maximum concentration of $87 \text{ mmol}\cdot\text{L}^{-1}$ at the same dilution rate while initial glycerol concentration is changed from 150 to $1550 \text{ mmol}\cdot\text{L}^{-1}$. The latter is closer to experimental results, indicating that two regulated negative-feedback mechanisms of 3-HPA are more appropriate for the *dha* regulon. 3-HPA accumulation was also observed for enterobacterial species, *i.e.* *K. pneumoniae*, *Citrobacter freundii* and *Enterobacter agglomerans*, where growth cessation and low product formation were evident [24, 25, 47]. The inhibition of GDH, GDHt and PDOR activities by 3-HPA was also investigated [10, 24, 25]. The mathematical model that considers the inhibitory effects of 3-HPA on activity of GDHt and PDOR showed that 3-HPA inhibits PDOR more than GDHt [22]. Thus the tolerance to the inhibition of 3-HPA should be strengthened.

Figure 9 shows that the computational results for the intracellular level of GDHt at various dilution rates and initial glycerol concentrations in continuous cultures of *K. pneumoniae*. The influences of dilution rate and initial glycerol concentration on the intracellular level of repressor mRNA, repressor, and GDHt and PDOR and their corresponding mRNAs are similar. Therefore, only the result for GDHt is shown as a representative. The levels of these substances decrease as the initial glycerol concentration increases at a fixed dilution rate. This indicates that 3-HPA accumulation is connected to the posttranslational decrease of the concentrations of the key enzymes in the reductive pathway of glycerol metabolism. At dilution rate of

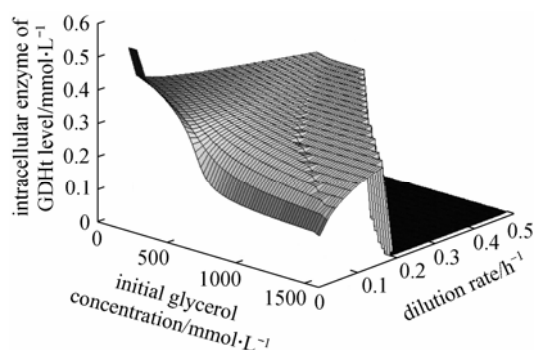


Figure 9 Computational results of intracellular GDHt levels at various dilution rates and initial glycerol concentrations for continuous cultures of *K. pneumoniae*

0.1 h^{-1} and increasing initial glycerol concentration, 3-HPA accumulates quickly until the initial glycerol concentration reaches about $1100 \text{ mmol}\cdot\text{L}^{-1}$. During this period, concentrations of repressor and key enzymes all decrease due to the toxicity from 3-HPA accumulation. Previous work has suggested that the 3-HPA toxicity could inhibit DNA synthesis [26]. It has been postulated that the reactivity of the aldehyde group of 3-HPA causes DNA damage similar to that exerted by formaldehyde [26]. Furthermore, other researches have indicated that accumulation of 3-HPA is associated with the instability of the plasmid bearing the *dhaB* genes [27]. These facts reveal that 3-HPA accumulation may repress the expression of the *dha* regulon to some extent at the transcriptional level.

Experimental studies have showed that the specific activities of GDHt and PDOR *in vitro* depend not only on cell growth, but also on the residual glycerol concentration in the bioreactor by *K. pneumoniae* [48]. Kinetic and pathway analysis suggest that GDHt is a major rate-limiting enzyme for the consumption of glycerol and for the formation of 1,3-PD by *K. pneumoniae* and *C. butyricum* [48, 49]. The specific activity of GDHt and PDOR are much lower compared with the specific activity of GDH. However, in the case of *K. pneumoniae*, the specific activities of these three enzymes show similar trends with respect to the effect of residual glycerol concentration and dilution rate [8]. As for *C. butyricum*, significant specific activity of PDOR ($0.4 \mu\text{mol}\cdot\text{min}^{-1}\cdot\text{mg}^{-1}$) and high levels of intracellular NADH were detected after a step change in dilution rate from 0.08 h^{-1} to 0.30 h^{-1} at glycerol feed concentration of $434 \text{ mmol}\cdot\text{L}^{-1}$ [49].

As indicated by the pathway of glycerol metabolism, PDOR catalyzes a reversible reaction. Ahrens *et al.* reported that the physiological forward reaction rate is four times the reverse reaction [48]. In a recent proteomic study, a hypothetical oxidoreductase (HOR) is identified in the later phase of fermentation by *K. pneumoniae*, which has 89% identity with the hypothetical oxidoreductase of *E. coli* (*yqhD*) that is induced by 3-HPA accumulation [50]. HOR is hypothesized to catalyze 3-HPA to 1,3-PD (replacing the function of PDOR), but with a much lower reverse step and therefore leads to less accumulation of 3-HPA. The production of 1,3-PD by modified strains [14-16] did not increase significantly compared to the production by wild-type strain. For example, GDHt and PDOR from *K. pneumoniae* were overexpressed in *E. coli* and $6.3 \text{ g}\cdot\text{L}^{-1}$ of 1,3-PD was obtained under fed-batch culture using glucose and glycerol as co-substrates [13, 51]. However, with the less extent of HOR to catalyze for the conversion of 1,3-PD back to 3-HPA, it may be more appropriate to overexpressed HOR (rather than PDOR) to drive the accumulated 3-HPA toward 1,3-PD formation, and thereby alleviating its toxicity to the cell.

4 CONCLUSIONS

In this study, an expanded mathematical model

was developed to describe the *dha* regulon of glycerol metabolism. Based on two regulated negative-feedback mechanisms of repression and enzyme inhibition, the expression of gene-mRNA-enzyme-product was investigated in details. The repressor and the two key enzymes, GDHt and PDOR, were all taken into account according to the repression of the *dha* regulon by 3-HPA. The transition from the mathematical model to the numerical S-system model was used to discuss the model robustness. The sensitivity analysis shows that the model is sufficiently robust. Moreover, multiplicity analysis for continuous cultures is developed, and its application to the regulation of the *dha* regulon reveals two regions of multiplicity. The range predicted for the occurrence of multiplicity agrees well with the experimental observations for the culture of *K. pneumoniae* grown on glycerol. The intracellular concentrations of glycerol, 1,3-PD, 3-HPA, repressor mRNA level, repressor level, and the enzymes of GDHt and PDOR and their mRNA level can be predicted for continuous cultures. The results of simulation and analysis indicate that the accumulation of intermediate 3-HPA will repress the expression of the *dha* regulon at transcriptional level. The strain presenting tolerance to the inhibition by 3-HPA should be strengthened and HOR should be overexpressed to accelerate the reversion of toxic accumulation of 3-HPA by re-directing it to the formation of 1,3-PD. This model gives new insights into the regulation of glycerol metabolism in *K. pneumoniae* and explains some experimental observations.

ACKNOWLEDGEMENTS

We thank Alan K. Chang for his help with the revision of the manuscript.

NOMENCLATURE

B	surface area of per biomass, $\text{mm}^2 \cdot \text{g}^{-1}$
C_{EtOH}	extracellular ethanol concentration, $\text{mmol} \cdot \text{L}^{-1}$
C_{HAc}	extracellular acetate concentration, $\text{mmol} \cdot \text{L}^{-1}$
$C_{\text{PDI}}, C_{\text{PDe}}$	intracellular and extracellular 1,3-propanediol concentrations, $\text{mmol} \cdot \text{L}^{-1}$
$C_{\text{so}}, C_{\text{se}}, C_{\text{si}}$	substrate (glycerol) concentration in feed medium, extracellular and intracellular glycerol concentration in reactor, $\text{mmol} \cdot \text{L}^{-1}$
C_{pi}^*	maximum product concentration ($\text{pi} = 1, 3\text{-PD, EtOH and HAc}$), $\text{mmol} \cdot \text{L}^{-1}$
C_{se}^*	maximum residual substrate concentration, $\text{mmol} \cdot \text{L}^{-1}$
$C_{3\text{-HPA}}$	intracellular 3-hydroxypropionaldehyde concentration, $\text{mmol} \cdot \text{L}^{-1}$
D	dilution rate, h^{-1}
D_{f}	diffusion coefficient of glycerol, $\text{L} \cdot \text{mm}^{-1} \cdot \text{h}^{-1}$
J_{max}	maximum specific transport rate of substrate, $\text{mmol} \cdot \text{g}^{-1} \cdot \text{h}^{-1}$
K_{m}	Michaelis-Menten constant of glycerol permease, $\text{mmol} \cdot \text{L}^{-1}$
$K_{\text{mGDHt}}, K_{\text{mPDOR}}$	Michaelis-Menten constant of enzymes of GDHt and PDOR, $\text{mmol} \cdot \text{L}^{-1}$
K_{PD}	diffusion coefficient for 1,3-PD of <i>K. pneumoniae</i> , h^{-1}

K_{s}	Monod saturation constant for substrate, $\text{mmol} \cdot \text{L}^{-1}$
$K_{\text{i}}^{\text{GDHt}}, K_{\text{i}}^{\text{PDOR}}$	inhibitor constant for 3-HPA to enzyme of GDHt and PDOR, $\text{mmol} \cdot \text{L}^{-1}$
$K_{\text{s}}^*, K_{\text{pi}}^*$	saturation constants for substrate and product in kinetic equations with excess terms ($\text{pi} = 1,3\text{-PD, EtOH and HAc}$), $\text{mmol} \cdot \text{L}^{-1}$
k_1, k_2	catalyze coefficient of GDHt for glycerol and PDOR for 3-HPA, h^{-1}
$m_{\text{ss}}, m_{\text{pi}}$	maintenance term of substrate consumption and product formation under substrate-limited conditions ($\text{pi} = 1,3\text{-PD, EtOH and HAc}$), $\text{mmol} \cdot \text{g}^{-1} \cdot \text{h}^{-1}$
$q_{\text{ss}}, q_{\text{pi}}$	specific rates of substrate uptake and product formation ($\text{pi} = 1,3\text{-PD, EtOH and HAc}$), $\text{mmol} \cdot \text{g}^{-1} \cdot \text{h}^{-1}$
$\Delta q_{\text{s}}^{\text{m}}, \Delta q_{\text{pi}}^{\text{m}}$	maximum increment of substrate consumption rate and product formation rate under substrate-sufficient conditions ($\text{pi} = 1,3\text{-PD, EtOH and HAc}$), $\text{mmol} \cdot \text{g}^{-1} \cdot \text{h}^{-1}$
t	time, h
V_{s}	specific intracellular volume in $\text{L} \cdot \text{g}^{-1}$ biomass
X	biomass concentration, $\text{g} \cdot \text{L}^{-1}$
Y_{pi}^{m}	product yield ($\text{pi} = 1,3\text{-PD, EtOH and HAc}$), $\text{mmol} \cdot \text{g}^{-1}$
Y_{s}^{m}	maximum growth yield, $\text{g} \cdot \text{mmol}^{-1}$
δ	cell membrane thickness, mm
μ, μ_{m}	specific and maximum specific growth rate, h^{-1}

REFERENCES

- Santillan, M., Zeron, E.S., "Analytical study of the multiplicity of regulatory mechanisms in the tryptophan operon", *Bull Math Biol*, **68** (2), 343–359 (2006).
- Xiu, Z.L., Song, B.H., Sun, L.H., Feng, E.M., Zeng, A.P., "Theoretical analysis of effects of metabolic overflow and time delay on the performance and dynamic behavior of a two-stage fermentation process", *Biochem Eng J*, **11**, 101–109 (2002).
- Mccoy, M., "Chemical makers try biotech paths", *Chem. Eng. News*, **76**, 13–19 (1998).
- Mu, Y., Teng, H., Zhang, D.J., Wang, Y.H., Xiu, Z.L., "Microbial production of 1,3-propanediol by *Klebsiella pneumoniae* using crude glycerol from biodiesel preparations", *Biotechnol Lett*, **28** (21), 1755–1759 (2006).
- Papanikolaou, S., Fick, M., Aggelis, G., "The effect of raw glycerol concentration on the production of 1,3-propanediol by *Clostridium butyricum*", *J Chem Tech Biotechnol*, **79**, 1189–1196 (2004).
- Deckwer, W.D., "Microbial conversion of glycerol into 1,3-propanediol", *FEMS Microbiol. Reviews*, **16**, 143–149 (1995).
- Gonzalez-Pajuelo, M., Andrade, J.C., Vasconcelos, L., "Production of 1,3-propanediol by *Clostridium butyricum* VPI 3266 in continuous cultures with high yield and productivity", *J Ind Microbiol Biotechnol*, **32** (9), 391–396 (2005).
- Sun, J.B., van den Heuvel, J., Soucaille, P., Qu, Y., Zeng, A.P., "Comparative genomic analysis of *dha* regulon and related genes for anaerobic glycerol metabolism in bacteria", *Biotechnol Prog*, **19** (2), 263–272 (2003).
- Biebl, H., Menzel, K., Zeng, A.P., Deckwer, W.D., "Microbial production of 1,3-propanediol", *Appl Microbiol Biotechnol*, **52** (3), 289–297 (1999).
- Wang, W., Sun J.B., Hartlep, M., Deckwer, W.D., Zeng, A.P., "Combined use of proteomic analysis and enzyme activity assays for metabolic pathway analysis of glycerol fermentation by *Klebsiella pneumoniae*", *Biotechnol Bioeng*, **83** (5), 525–536 (2003).
- Zeng, A.P., Biebl, H., "Bulk chemicals from biotechnology: The case of 1,3-propanediol production and the new trends", *Adv Biochem Eng Biotechnol*, **74**, 239–259 (2002).
- Forage, R.G., Lin, E.C., "DHA system mediating aerobic and anaerobic dissimilation of glycerol in *Klebsiella pneumoniae* NCIB 418", *J Bacteriol*, **151** (2), 591–599 (1982).
- Tong, I.T., Liao, H.H., Cameron, D.C., "1,3-Propanediol production by *Escherichia coli* expressing genes from the *Klebsiella pneumoniae*

- dha* regulon", *Appl Environ Microbiol*, **57** (12), 3541–3546 (1991).
- 14 Sprenger, G.A., Hammer, B.A., Johnson, E.A., Lin, E.C., "Anaerobic growth of *Escherichia coli* on glycerol by importing genes of the *dha* regulon from *Klebsiella pneumoniae*", *J Gen Microbiol*, **135** (5), 1255–1262 (1989).
- 15 Tong, I.T., Cameron, D.C., "Enhancement of 1,3-propanediol production by cofermentation in *Escherichia coli* expressing *Klebsiella pneumoniae dha* regulon genes", *Appl Biochem Biotechnol*, **34**, 149–159 (1992).
- 16 Toraya, T., "Radical catalysis of B12 enzymes: Structure, mechanism, inactivation, and reactivation of diol and glycerol dehydratases", *Cell Mol Life Sci*, **57** (1), 106–127 (2000).
- 17 Tran-Dinh, K., Hill, F.F., "A method for the preparation of 1,3-propanediol", German Pat., No. DE 3734764 A1 (1987).
- 18 Zeng, A.P., "A kinetic model for product formation of microbial and mammalian cells", *Biotechnol. Bioeng.*, **46**, 314–324 (1995).
- 19 Zeng, A.P., Byun, T.G., Posten, C., Deckwer, W.D., "Use of respiratory quotient as a control parameter for optimum oxygen supply and scale-up of 2,3-butanediol production under microaerobic conditions", *Biotechnol. Bioeng.*, **44** (9), 1107–1114 (1994).
- 20 Zeng, A. P., Deckwer, W.D., "A kinetic model for substrate and energy consumption of microbial growth under substrate-sufficient conditions", *Biotechnol Prog*, **11** (1), 71–79 (1995).
- 21 Xiu, Z.L., Zeng, A.P., An, L.J., "Mathematical modeling of kinetics and research on multiplicity of glycerol bioconversion to 1,3-propanediol", *J. Dalian Univ. Technol.*, **40**, 428–433 (2000).
- 22 Sun, Y.Q., Qi, W.T., Teng, H., Xiu, Z.L., Zeng, A.P., "Mathematical modeling of glycerol fermentation by *Klebsiella pneumoniae*: Concerning enzyme-catalytic reductive pathway and transport of glycerol and 1,3-propanediol across cell membrane", *Biochem. Eng. J.*, **38**, 22–32 (2008).
- 23 Zeng, A.P., "Quantitative cell physiology, metabolic engineering and modeling of the glycerol fermentation to 1,3-propanediol, habilitation", Ph.D. Thesis, Technical University of Braunschweig, Germany (2000).
- 24 Barbirato, F., Grivet, J.P., Soucaille, P., Bories, A., "3-Hydroxypropionaldehyde, an inhibitory metabolite of glycerol fermentation to 1,3-propanediol by enterobacterial species", *Appl Environ Microbiol*, **62** (4), 1448–1451 (1996).
- 25 Barbirato, F., Soucaille, P., Bories, A., "Physiologic mechanisms involved in accumulation of 3-hydroxypropionaldehyde during fermentation of glycerol by *Enterobacter agglomerans*", *Appl Environ Microbiol*, **62** (12), 4405–4409 (1996).
- 26 Rasch, M., "The influence of temperature, salt and pH on the inhibitory effect of reuterin on *Escherichia coli*", *Int J Food Microbiol*, **72** (3), 225–231 (2002).
- 27 Zheng, P., Wereath, K., Sun, J.B., Heuvel, J., Zeng, A.P. "Overexpression of genes of the *dha* regulon and its effects on cell growth, glycerol fermentation to 1,3-propanediol and plasmid stability in *Klebsiella pneumoniae*", *Process Biochemistry*, **41**, 2160–2169 (2006).
- 28 Sinha, S., "Theoretical study of tryptophan operon: Application in microbial technology", *Biotechnol. Bioeng.*, **31** (2), 117–124 (1988).
- 29 Bachler, C., Schneider, P., Bahler, P., Lustig, A., Erni, B., "*Escherichia coli* dihydroxyacetone kinase controls gene expression by binding to transcription factor DhaR", *Embo J*, **24** (2), 283–293 (2005).
- 30 Daniel, R., Boenigk, R., Gottschalk, G., "Purification of 1,3-propanediol dehydrogenase from *Citrobacter freundii* and cloning, sequencing, and overexpression of the corresponding gene in *Escherichia coli*", *J. Bacteriol.*, **177**, 2151–2156 (1995).
- 31 Zeng, A.P., Rose, A., Biebl, H., Tag, C., Guenzel, B., Deckwer, W.D., "Multiple product inhibition and growth modeling of *Clostridium butyricum* and *Klebsiella pneumoniae* in glycerol fermentation", *Biotechnol. Bioeng.*, **44**, 902–911 (1994).
- 32 Menzel, K., Zeng, A.P., Deckwer, W.D., "High concentration and productivity of 1,3-propanediol from continuous fermentation of glycerol by *Klebsiella pneumoniae*", *Enzyme Microbiol. Technol.*, **20**, 82–86 (1997).
- 33 Torres, V.N., Voit, E., *Pathway Analysis and Optimization in Metabolic Engineering*, Cambridge University Press, Cambridge (2002).
- 34 Marin-Sanguino, A., Torres, N.V., "Optimization of tryptophan production in bacteria. Design of a strategy for genetic manipulation of the tryptophan operon for tryptophan flux maximization", *Biotechnol. Prog.*, **16** (2), 133–145 (2000).
- 35 Menzel, K., Zeng, A.P., Biebl, H., Deckwer, W.D., "Kinetic, dynamic, and pathway studies of glycerol metabolism by *Klebsiella pneumoniae* in anaerobic continuous culture: I. The phenomena and characterization of oscillation and hysteresis", *Biotechnol. Bioeng.*, **52** (5), 549–560 (1996).
- 36 Xiu, Z.L., Zeng, A.P., Deckwer, W.D., "Multiplicity and stability analysis of microorganisms in continuous culture: Effects of metabolic overflow and growth inhibition", *Biotechnol. Bioeng.*, **57** (3), 251–261 (1998).
- 37 Zeng, A.P., Menzel, K., Deckwer, W.D., "Kinetic, dynamic, and pathway studies of glycerol metabolism by *Klebsiella pneumoniae* in anaerobic continuous culture: II. Analysis of metabolic rates and pathways under oscillation and steady-state conditions", *Biotechnol. Bioeng.*, **52** (5), 561–571 (1996).
- 38 Xiu, Z.L., Song, B.H., Wang, Z.T., Sun, L.H., Feng, E.M., Zeng, A.P., "Optimization of biodissimilation of glycerol to 1,3-propanediol by *Klebsiella pneumoniae* in one- and two-stage continuous anaerobic cultures", *Biochem. Eng. J.*, **19**, 189–197 (2004).
- 39 Ma, Y.F., Sun, L.H., Xiu, Z.L., "Microbial theoretical analysis of oscillatory behavior in process of microbial continuous culture", *Chin J Eng Math*, **20**, 1–6 (2003).
- 40 Ye, J.X., Feng, E.N., Lian, H.S., Xiu, Z.L., "Existence of equilibrium points and stability of the nonlinear dynamical system in microbial continuous cultures", *Applied Mathematics and Computation*, **207**, 307–318 (2008).
- 41 Biebl, H., Marten, S., Hippe, H., Deckwer, W.D., "Glycerol conversion to 1,3-propanediol by newly isolated *Clostrida*", *Appl. Microbiol. Biotechnol.*, **36**, 592–597 (1992).
- 42 Homann, T., Tag, C., H B, Deckwer, W.D., Schink, B., "Fermentation of glycerol to 1,3-propanediol by *Klebsiella* and *Citrobacter* strains", *Appl Microbiol Biotechnol*, **33**, 121–126 (1990).
- 43 Chen, X., Xiu, Z.L., Wang, J.F., Zhang, D.J., Xu, P., "Stoichiometric analysis and experimental investigation of glycerol conversion to 1,3-propanediol by *Klebsiella pneumoniae* under microaerobic conditions", *Enzyme Microbiol. Technol.*, **33**, 386–394 (2003).
- 44 Papanikolaou, S., Ruiz-Sanchez, P., Pariset, B., Blanchard, F., Fick, M., "High production of 1,3-propanediol from industrial glycerol by a newly isolated *Clostridium butyricum* strain", *J. Biotechnol.*, **77** (2-3), 191–208 (2000).
- 45 González-Pajuelo, M., Andrade, J., Vasconcelos, I., "Production of 1,3-propanediol by *Clostridium butyricum* VPI 3266 using a synthetic medium and raw glycerol", *J Ind Microbiol Biotechnol*, **31**, 442–446 (2004).
- 46 Gonzalez-Pajuelo, M., Meynial-Salles, I., Mendes, F., Andrade, J. C., Vasconcelos, I., Soucaille, P., "Metabolic engineering of *Clostridium acetobutylicum* for the industrial production of 1,3-propanediol from glycerol", *Metab Eng*, **7** (5-6), 329–336 (2005).
- 47 Barbirato, F., Soucaille, P., Camarasa, C., Bories, A., "Uncoupled glycerol distribution as the origin of the accumulation of 3-hydroxypropionaldehyde during the fermentation of glycerol by *enterobacter agglomerans* CNCM 1210", *Biotechnol. Bioeng.*, **58** (2-3), 303–305 (1998).
- 48 Ahrens, K., Menzel, K., Zeng, A.P., Deckwer, W.D., "Kinetic, dynamic, and pathway studies of glycerol metabolism by *Klebsiella pneumoniae* in anaerobic continuous culture: III. Enzymes and fluxes of glycerol dissimilation and 1,3-propanediol formation", *Biotechnol. Bioeng.*, **59**, 544–552 (1998).
- 49 Abbad-Andaloussi, S., Guedon, E., Spiesser, E., Petttdemange, H., "Glycerol dehydratase activity: the limiting step for 1,3-propanediol production by *Clostridium butyricum* DSM5431", *Lett. Appl. Microbiol.*, **22**, 311–314 (1996).
- 50 Wang, W., Sun, J.B., Nimtz, M., Deckwer, W.D., Zeng, A.P., "Protein identification from two-dimensional gel electrophoresis analysis of *Klebsiella pneumoniae* by combined use of mass spectrometry data and raw genome sequences", *Proteome Sci*, **1** (1), 525–536 (2003).
- 51 Skraly, F.A., Lytle, B.L., Cameron, D.C., "Construction and characterization of a 1,3-propanediol operon", *Appl Environ Microbiol*, **64** (1), 98–105 (1998).